Measurement of vocal fold intraglottal pressure and impact stress

Article *in* Journal of Voice · July 1994

DOI: 10.1016/S0892-1997(05)80305-4 · Source: PubMed

2 authors:

Jack J Jiang
University of Wisconsin–Madison

Ingo R Titze
University of Utah

Journal of Voice
Vol. 8, No. 2, pp. 132–144

Measurement of Vocal Fold Intraglottal Pressure and Impact Stress

Jack Jiaqi Jiang and Ingo R. Titze

Voice Acoustics and Biomechanics Laboratory, Department of Speech Pathology and Audiology, and National Center for Voice and Speech, University of Iowa, Iowa City, Iowa, U.S.A.

Summary: Intraglottal pressure was measured according to a previously described hemilarynx procedure. Three phases were identified for intraglottal pressure: an impact phase, in which the vocal folds come into contact and produce a sharp pressure pulse; a preopen phase, in which there is a progressive pressure buildup due to increased exposure of the vocal fold surfaces to subglottal pressure; and an open phase, in which intraglottal pressure becomes aerodynamic and drops gradually from opening to closing. Impact pressure peaks were positively related to subglottal pressure, elongation, and adduction of the vocal folds. The midpoint of the membranous vocal fold received the maximum impact stress. The experimental results match well with analytical predictions and support a current theory of mechanical trauma leading to vocal nodules. **Key Words:** Mechanical stress—Trauma—Nodules—Voice disorders—Hyperadduction.

Impact stress on vocal fold tissues is an important variable for understanding the mechanism of phonation and for determining the etiology of vocal nodules. The purpose of the present experiment was to measure impact stress in conjunction with aerodynamic pressure in the glottis of an excised hemilarynx (1). Impact stress was defined as the normal (perpendicular) stress on the contacting surfaces of the vocal folds. The stress component parallel to the surface (the shear stress) was ignored. Aerodynamic pressure was defined as the pressure on a vocal fold surface point when there is contact only with air. The following relations were investigated: (a) impact stress and aerodynamic pressure versus subglottal pressure; (b) impact stress and aerodynamic pressure versus prephonatory configuration; (c) impact stress versus vocal fold elongation; and (d) spatial distribution of impact stress on the vocal fold.

To bring the measurement of impact stress into a historical perspective, a brief sketch of previous attempts to measure intraglottal pressure is presented.

BACKGROUND ON INTRAGLOTTAL PRESSURE MEASUREMENT

Intraglottal pressure is the driving pressure for vocal fold vibration. Its observation in conjunction with vocal fold movement, vocal fold contact area, and acoustic pressure is essential to a full understanding of the mechanism of phonation.

Accompanying the development of a phonation theory, there have been a series of experiments measuring intraglottal pressure. During the 19th century, the study of laryngeal aerodynamics was approached on the basis of either physical models or experiments with excised larynges. According to Cooper (2), Harless (3) expressed regret that ma-

Accepted May 12, 1993.

Address correspondence and reprint requests to Dr. I. R. Titze at Voice Acoustics and Biomechanics Laboratory, Department of Speech Pathology and Audiology, University of Iowa, 330-WJSHC, Iowa City, IA 52242, U.S.A.

Dr. J. J. Jiang's current address is Department of Otolaryngology/Head and Neck Surgery, Northwestern University, Chicago, IL, U.S.A.

nometers did not have the high-frequency response necessary to measure the dynamic variation of laryngeal air pressures during the glottal cycle; however, Harless hypothesized negative air pressures in the lower part of the glottis ("immediately below the fold") when the vocal folds were approaching each other at narrow glottal widths. In 1925, Tonndorf [cited in Cooper (2)] studied the Bernoulli principle with excised bovine larynges and found that, besides regions of strong positive pressure, there were also regions of strong negative pressure. According to Cooper, Weiss (4) published the first simultaneous cycle-to-cycle records of dynamic subglottal pressures. Weiss also recorded medial–lateral movement of the vocal folds by shining a narrow beam of light through the glottis, resulting in an image that permitted separate observation of the movement of right and left vocal folds.

Rethi (1897; cited in ref. 5) placed a pressure-measuring elastic instrument into the glottis of animals and stimulated the cricothyroid and posterior cricoarytenoid muscles. The highest static pressures were estimated to be ~75 kPa (≈750 cm H_2O). Kakeshita (1927; cited in ref. 5) placed an inflatable rubber balloon within the glottis of canines and obtained pressures >53 kPa during barking. Murakami and Kirchner (6,7) used a low-frequency pressure catheter between the vocal folds of cats to measure pressure changes due to nerve stimulation. The largest pressure variation measured was only ~1.68 kPa, which is closer to the dynamic variations that will be described in this study.

Scherer and Titze (8) placed a miniature transducer between the vocal processes of an excised bovine larynx and found that the maximum variation in contact pressure during phonation ranged from values less than the average subglottal pressure to values twice as large as the average subglottal pressure. In particular, the within-cycle variation of interarytenoid pressure was 1.5–11.3 kPa. Their results showed a positive relationship between peak-to-peak variations in interarytenoid pressure and mean subglottal pressure.

More recently, Reed et al. (9) obtained an intraglottal pressure waveform from a human volunteer. The waveform was similar to that reported by Scherer et al., namely, a pronounced initial peak and a long, rounded segment. Reed et al. also found that there is a clear increase in the output of the intraglottal transducer with increases in the amplitude of the acoustic signal.

According to these studies, it would seem that current knowledge of intraglottal pressures would be advanced by a more systematic study that quantifies the relation between intraglottal pressure and phonatory control variables such as lung pressure, adduction, fundamental frequency, and mode of phonation.

BACKGROUND ON THE ETIOLOGY OF VOCAL NODULES

Vocal nodules are the most common vocal disorders. They represent 2–3.9% of the entire ENT case load (10). Since Terce first described the condition in 1868, discussion of etiology, histological nature, and therapy regarding vocal nodules has not ceased (11,12).

Chiari (1895; cited in ref. 13) and Epstein et al. (14) stressed the mechanical nature of the origin of nodules. These pathologic growths are now generally considered to be the consequence of mechanical trauma. A number of hypotheses have been proposed to explain the cause of vocal nodules and polyps (15). However, no supporting data are strong enough to be used as evidence for the mechanical trauma hypothesis. The mechanical effects of vibration of vocal folds should be measured directly to clarify their influence on the tissue microstructure during phonation.

The following three hypotheses have been proposed regarding the types of mechanical influences that may be important.

1. Mechanical pressure hypothesis. According to Arnold (16,17) nodules are the result of faulty or excessive vocal use. They may be likened to calluses on the hand or corns on the toes, the result of mechanical stress applied by tools or tight shoes. Sonninen et al. (15) hypothesized that microtrauma is more likely to be caused by pressing forces ("hammer-and-anvil mechanism"). Vaughan (18) stated that vocal nodules develop from mechanical trauma caused by one vocal fold rubbing against the other. These authors all agree on the direct mechanical cause of hyperkinetic phonatory movements.

2. Mechanical lifting hypothesis. Gery (19) stated that vocal nodules and polyps that occur at the junction of the anterior and middle thirds of the folds are due to mucosal distortion on separation (lifting of the cover) and not to the trauma of collision. As the vocal folds abduct, a triangular wedge of mucous membrane forms. As the folds further abduct, this triangular wedge is the last point to separate and

corresponds to the site of vocal nodules. As the process continues, the mucous membrane thickens, and eventually nodules occur.

3. Accumulation hypothesis. By using a mathematical analysis and a physical model of vocal fold vibration, Jiang (20) found that the liquid on a vibrating band tends to accumulate toward the midpoint of the band. Clinically, vocal fold nodules also tend to occur at the midmembranous fold. Combining the equation of fluid motion with the dynamics of string vibration, it was shown that fluid pressures build up toward the center of the vocal folds and that mechanical stresses may result from fluid accumulation.

Although all three hypotheses involve the claim that mechanical stress is the key to the etiology of vocal nodules, accurate measurement of such a stress has not been accomplished. The measurements presented here will help to set the stage for eventual formal testing of these hypotheses.

BIOMECHANICAL ANALYSIS AND PREDICTION OF IMPACT STRESS

According to the body-cover theory (21,22), the vocal fold cover can be modeled as a vibrating ribbon. The mass M of a small element near the surface is

$$M = \rho dxdydz \tag{1}$$

where ρ is the tissue density and dx, dy, dz are spatial increments. Assuming the lateral displacement ξ of the tissue element to be sinusoidal in time during the open phase of the glottal cycle, then

$$\xi = A\sin 2\pi ft \qquad 0 < t < \frac{1}{2f} \tag{2}$$

where A is the displacement amplitude, f is the frequency of vibration, and the open phase is assumed to be half the vibratory period. The velocity of the element (the time derivative of ξ) will then be

$$v = 2\pi fA\cos 2\pi ft \tag{3}$$

Now consider Newton's second law of motion (force equals mass times acceleration) in terms of a mean impact force F distributed over an impact interval of time Δt. Then,

$$F\Delta t = m\Delta v \tag{4}$$

where Δv is the change in velocity during the impact.

If we define the beginning of impact as the moment of peak velocity ($v = 2\pi fA$) and the end of impact as the moment of zero velocity, then $\Delta v = 2\pi fA$, and the mean impact force is

$$F = \frac{(\rho dxdydz)(2\pi fA)}{\Delta t} \tag{5}$$

If the impact force is evenly distributed over the vocal fold surface area $dydz$, the mean contact stress (pressure) on the element is

$$P = \frac{(\rho dx)(2\pi fA)}{\Delta t} \tag{6}$$

The thickness dx of vibrating tissue is assumed to be on the order of 0.1 cm (23), and typical amplitudes of vibration are also on the order of 0.1 cm. For a fundamental frequency of 200 Hz (covering both the male and the female range), a tissue density of 1.0 g/cm^3 and a Δt of 0.5 ms (as measured typically in this experiment), the predicted mean contact stress is on the order of 3.0 kPa.

If the anterior–posterior (y) variation of the ribbon-like displacement during the impact of the two vocal folds resembles a half-sinusoid (1,24), then

$$P(y) = \left(\frac{2\pi\rho dxAf}{\Delta t}\right)\sin\left(\frac{\pi y}{L}\right) \tag{7}$$

Note that the predicted stress is proportional to vibrational amplitude and frequency. Note also that the predicted stress reaches its maximum at the midpoint of the membranous fold ($y = L/2$). At the $L/4$ and $3L/4$ points, the contact stress is

$$P_{1/4} = P_m\sin\left(\frac{\pi}{4}\right) \tag{8}$$

or ~70.7% of the maximum contact stress P_m at the midpoint. We now describe some methods for testing these relations experimentally.

METHODS

Biological tissue

Experimental data were obtained on five canine larynges. In addition, for normalized peak contact pressure measures, data from four canine larynges used previously (1) were included because these normalized data did not require a pressure and flow calibration. All larynges were harvested from 25- to 30-kg healthy mongrel dogs killed for other experimental purposes. No animals were killed for these experiments. There was no regard for sex or age of the animal. All larynges were examined visually by an otolaryngologist to reject any with pathology.

Instrumentation, calibration, and data recording

Details of the hemilarynx preparation procedure, subglottal system, mounting apparatus, strobe light illumination, and audio and video recording systems are described elsewhere (1). It was demonstrated that the hemilarynx, with a glass plate replacing one vocal fold, is a valid substitute for the whole larynx with regard to vibration pattern, vibrational amplitude, fundamental frequency, and airflow pattern. The magnitude of the airflow is scaled down by a factor of 2, however. This is predictable and does not affect the use of the hemilarynx for impact pressure studies. A brief synopsis of the hemilarynx procedure follows.

An apparatus was constructed with which vibration of an excised hemilarynx could be observed from the customary superior aspect (Fig. 1). The left half of the larynx was removed and replaced by a vertically oriented Plexiglas plate, held in place by two screws (top and bottom) as shown. Some additional mounting screws underneath the plate are seen shining through the plate. A three-pronged positioning device (right side in middle of Fig. 1) was used to adjust the position of the arytenoid cartilage of the vocal fold. For adjustment of vocal fold length, a rod was connected via a 90° crossarm and sutured to the anterior tip of the thyroid cartilage (top right of Fig. 1). The apparatus included instrumentation for recording and measuring the position of several observable landmarks (note three tiny black dots on vocal fold edge). Instrumentation for measurement of contact area profiles, intraglottal pressure, and contact stress is not shown for clarity.

The vertically oriented Plexiglas plate, custom built for every larynx, was modified from a design used previously (1). Three holes were drilled into the plate, in line with expected vocal fold contact locations (Fig. 2, plate tilted to see holes from vocal fold side). The opening of the middle hole faced the midpoint of the membranous vocal fold. The opening of the anterior and posterior holes faced the one-fourth anterior and one-fourth posterior points on the membranous vocal fold. An Entran miniature pressure transducer (EPB-125-5) was mounted

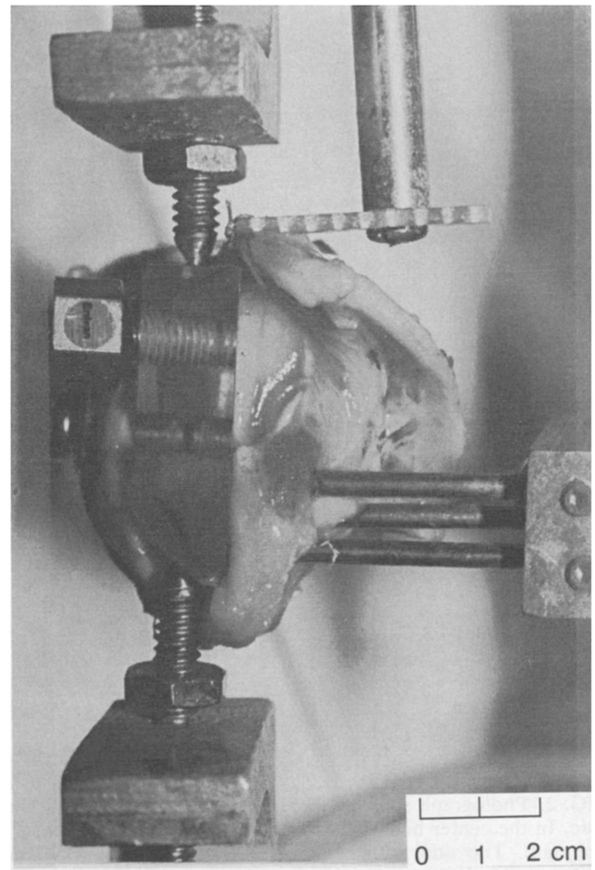

FIG. 1. Photograph showing top view of the hemilarynx and vertically oriented Plexiglas plate. The right vocal fold is abutted against the plate, which is mounted by two screws (top and bottom). Additional mounting screws are shining through the plate from below. A three-pronged device (middle right) is used to adjust the arytenoid cartilage, and a rod (upper right) is used to adjust the vocal fold length.

in one of these holes (the middle one in Fig. 2) to measure the contact stress at any of the three locations. When one hole was in use, the other two holes were sealed with a modified flat-end drill bit (seen as black rods in figure).

The stress-sensitive stainless-steel diaphragm of the transducer and the flat end of a machine screw were flush with the surface of the vertical plate so that the vocal fold side of the vertical plate had a continuous flat surface. The effective stress-sensitive diaphragm surface was <7 mm^2, which is less than a typical maximum vocal fold contact area (10 mm length $\times$ 3 mm depth $=$ 30 mm^2). The surface area could therefore be approximated as a "broad point" of contact between the vocal fold and the diaphragm. During vibration, the rise time of initial contact was typically $\sim$0.5 ms, based on the measurements with a Data 6000 digital signal

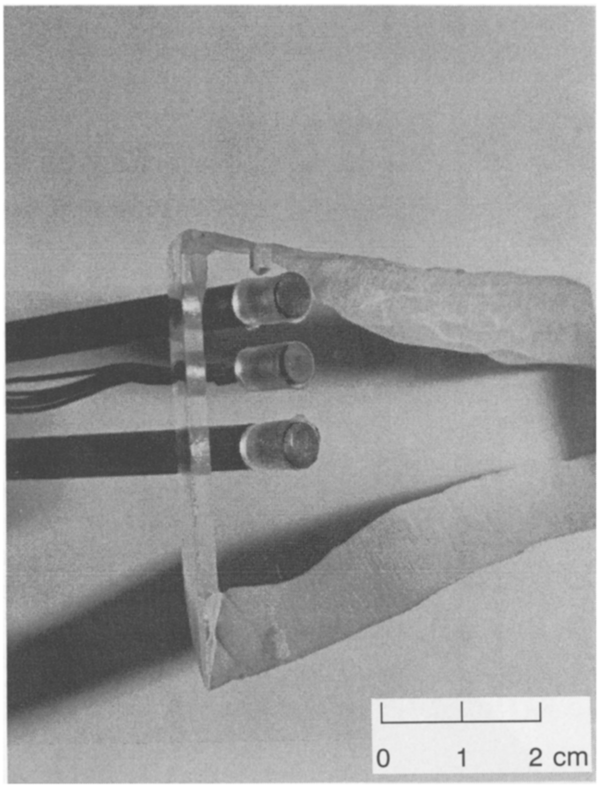

FIG. 2. Photograph showing Plexiglas plate from the vocal fold side. In the center hole is the stress-sensitive stainless-steel diaphragm. Top and bottom holes are plugged with machine screws and rods inserted at the same depth, making a continuous flat surface.

analyzer. This rise time is small in relation to a typical 10-ms fundamental period of vibration (100 Hz). Thus, both temporal and spatial resolutions of contact stress were obtained, although temporal resolution was much higher.

A sphygmomanometer (Nissei D-267038) was used to calibrate the Entran pressure transducer. The DC calibration result is shown in Fig. 3. The pressure signal was displayed and measured on the screen of a Data 6000 universal digital waveform analyzer. Since the frequency response of the combined transducer and amplifier (Entran IMV-15) was linear (less than ±0.5 dB) from DC 40 kHz according to the technical specifications of the manufacturer, separate AC calibration was not considered necessary.

According to spectral analysis done on the Data 6000 signal analyzer, the frequency spectrum of the AC portion of the pressure waveform was 50 Hz–10 kHz. This is not only within the manufacturer's frequency response specifications of the transducer, but also within the range of the Hi-Fi audio channels of a Panasonic 1960 VCR, which was used to record the AC portion of the signal. At least four audio channels were needed for recording the following signals: microphone, pressure waveform, strobe flash, and chatter signal. Since the VCR had only two audio channels, a 2 × 2 switch was used to select the appropriate channels. During the experiment, one switch combination was used to record a segment of phonation with two signals, then another combination was used to record a second segment with two other signals. Phase locking of all signals was obtained by combining first strobe flash with contact pressure, then contact pressure with microphone pressure. The synchronization error between the two audio channels was <0.05 ms.

Because the pressure sensor was made of semiconductive material, there was a significant baseline drift of pressure over time. This was caused by temperature changes and variable moisture conditions from the humidified air. Such a baseline drift was not recorded by the VCR, but could be monitored on-line by the Data 6000. When the equipment was warmed up (>30 min) and the baseline was reset between trials (when the airflow stopped), the typical baseline shift over 5–10 s was <10% of the peak-to-peak signal. A relatively dependable zero pressure baseline was maintained if the pressure waveform was recorded within this duration (R. C. Scherer, 1990, personal communication).

For visual observation, the top of the vertical plate was ground to form a prism to increase the

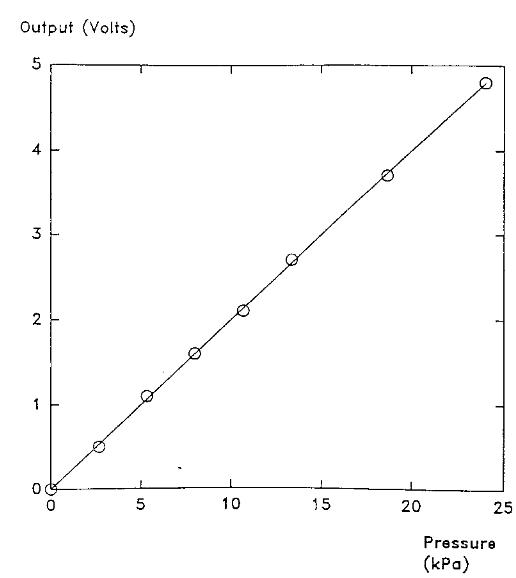

FIG. 3. Calibration for the Entran EPB-125-5 pressure transducer by use of a sphygmomanometer (Nissei D-267038).

contrast between contact and noncontact regions. The principle is illustrated in Fig. 4. Stroboscopic illumination (Pioneer DS-303) was introduced at surface A, which was at 45° from surface B. If the medium on the right side of B is low-density air, total reflection occurs because Plexiglas has a higher-density medium than air. However, if a wet vocal fold makes contact with surface B, the density of water is close to the density of the Plexiglas and total reflection does not occur; therefore, light penetrates surface B and illuminates the contact region, which becomes bright and easily identifiable with scattered light received at 90° to the surface. The principle of total reflection versus partial reflection and partial transmission worked well for this experiment. To keep the vocal fold wet, saline was dropped onto the tissue during the experiment.

MEASUREMENT AND DATA ANALYSIS

Pressure waveforms were displayed on the Data 6000 signal analyzer, either directly from the transducer–amplifier or from the audio channels of the VCR. They were also plotted on an HP 7475A Plotter. Any DC baseline of the pressure waveform

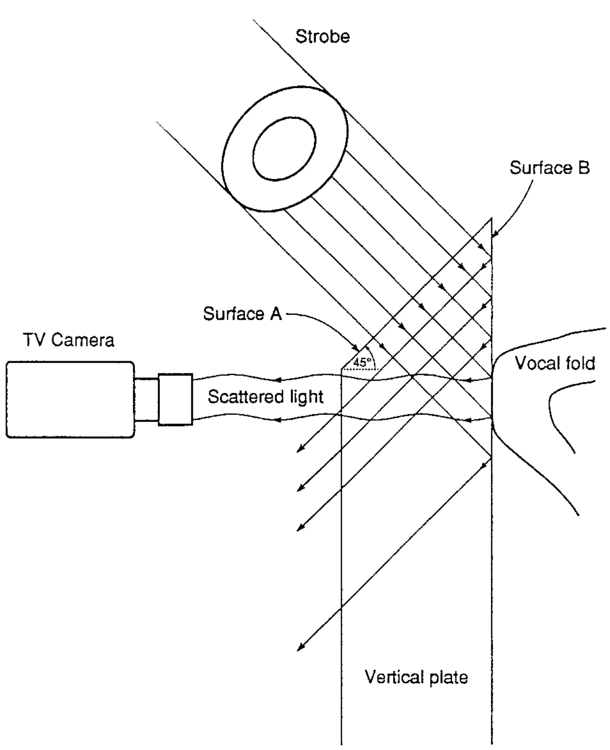

FIG. 4. Schematic showing the principle of illumination of the contact area. The illumination strobe light (Pioneer DS-303) is introduced at surface A, which is cut at 45° from surface B.

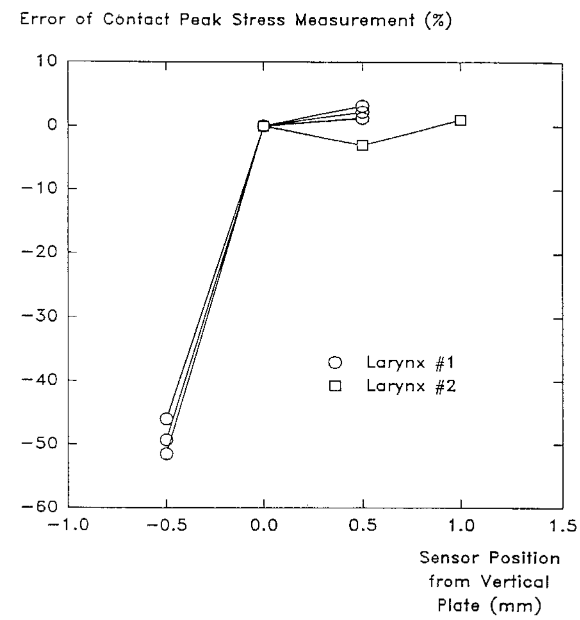

FIG. 5. Measurement error versus sensor position from the vertical plate. The peak impact stresses were normalized to the contact stress flush with the surface of the vertical plate (measurements were made on two larynges).

could be measured only if records came directly from the transducer–amplifier.

Peak stress was measured from the screen of the Data 6000. The stability of the peak stress was estimated on the basis of five repeated measurements in a single larynx. The measurement error was found to be <5%. The measurement of peak stress was dependent on the relative depth (flushness) of the sensor diaphragm with respect to the surface of the vertical plate, as shown in Fig. 5. The results show that the error was <5% when the diaphragm of the sensor was between 0.0 and 0.5 mm above the surface of the plate. Recessed (negative) positions gave erroneous results. The test was partially repeated for a second larynx, as shown. Prior to data collection, the surface was examined for each larynx to make certain that the sensor position was within the 0.0- to 0.5-mm tolerance.

Vocal fold elongation was measured from the distance between the anterior and posterior stitch marks on the screen of the video monitor (these were the small dots shown in Fig. 1). All the length measurements were normalized with respect to an initial elongation L_0 between anterior and posterior stitch marks. To define the L_0, the vocal fold adducted by forceps and the vocal fold length were measured before mounting. This length was also used for making or selecting the custom-built Plex-

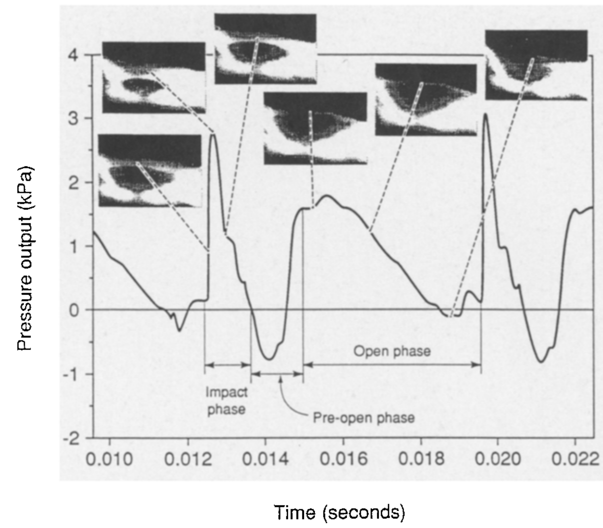

FIG. 6. Typical intraglottal pressure waveform with corresponding contact profiles in normal voice. Shim size was 0.5 mm and subglottal pressure was 1.96 kPa.

iglas plate. The purpose of length normalization was to reduce the effect of individual size differences in the larynges.

Vocal fold adduction was determined by the distance between the arytenoid cartilages. In this experiment, the distance was controlled by placing various sizes of wooden shims between the arytenoid cartilages. The adductive position against the shim was maintained constant by a micrometer so that thicker shims caused less adduction. The thickness of the wood shim was used as a parameter to represent the degree of adduction. A "negative" shim size was defined as an overshooting of the micrometer after it passed the controlled standard position. This overshooting was measured in micrometer units. Typically, both subglottal pressure and elongation had their greatest ranges when the shim size was 0.5 mm. Phonation at this setting was "optimal" in that it was stable, loud, and in modal register. This setting was called the standard setting and was used to normalize vocal fold adduction. There were three adduction conditions in this study: the standard setting; the standard setting plus 1 mm adduction (for which the "shim size" was −0.5 mm); and the standard setting minus 1 mm adduction (for which shim size was 1.5 mm).

The relation between peak stress and location of contact on the vocal fold was observed during optimal phonation, when the subglottal pressure was 1.2–1.6 kPa. Because of the large variation of this peak stress among trials and across larynges, each measured pressure was normalized to the peak stress at the midpoint of the vocal fold. Two normalized peak stresses, corresponding to anterior and posterior positions on vocal fold, were then studied.

RESULTS AND DISCUSSION

Intraglottal pressure waveforms and vocal fold movement

Figure 6 shows a typical waveform with corresponding contact profiles, and Fig. 7 shows the same waveform with sketches of the vocal fold in coronal view. These two figures will be discussed side by side. Based on simultaneous observations of vocal fold contact conditions with a vertical plate and sensor, the intraglottal pressure waveform was classified as having three phases: impact phase, preopen phase, and open phase.

The impact phase occurred when the vocal fold first made contact with the vertical plate and pressure sensor. Normal stress between the vocal fold and the vertical plate (or pressure sensor) rose quickly and assumed a peak value of ~3.0 kPa. This segment of the intraglottal pressure waveform was called impact stress. The impact phase finished with a quick stress relaxation, seen as a quick reduction in pressure just after the peak. This reduction refers biomechanically to a redistribution of tissue, i.e., a vertical "squishing" in which local internal stresses equalize.

The preopen phase occurred when the bottom lip of the vocal fold initiated separation and the top lip was still in contact with the vertical plate. In this phase, a buildup of intraglottal pressure resulted

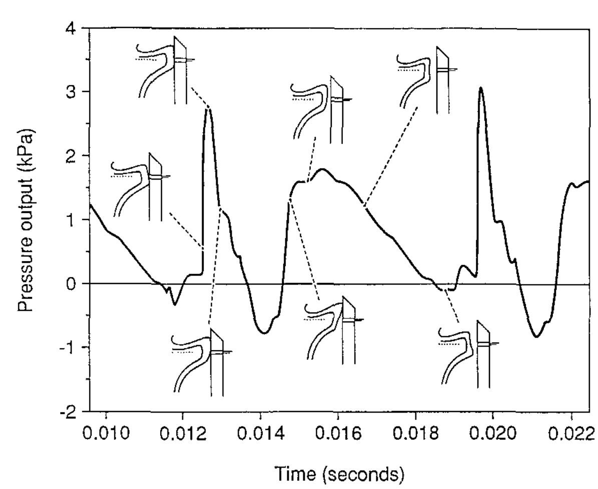

FIG. 7. Typical intraglottal pressure waveform with sketches of corresponding vocal fold movement in coronal plane. Shim size was 0.5 mm and subglottal pressure was 1.96 kPa.

from subglottal pressure being applied to the tissue, starting from the bottom and ending at the top lip of the vocal fold. The glottal shape was convergent in this phase. The preopen phase ended with another large positive intraglottal pressure, in which the pressure sensor had no contact with the vocal fold and the pressure waveform represented subglottal pressure.

The opening phase occurred when vocal fold had no more contact with the vertical plate. This phase started with the opening of the top lip of the vocal fold. Pressure dropped over most of this phase. At the end of this phase, just before the peak stress of the next cycle, the pressure was slightly negative. Much has been made in the literature about this negative (Bernoulli) pressure, but its importance is sometimes overstated.

Scherer and Titze (8) and Reed et al. (9) reported a similar pressure waveform from a full larynx, namely, an initial peak and a long, round segment. However, the segment of the preopen phase in their results was different from that shown in Figs. 6 and 7. Both groups of investigators showed a slower pressure buildup in this phase. Since previous methodologies consisted of inserting a pressure probe into the glottis, the possibility for leakage flow around the probe existed. Incomplete closure at the top lip may have caused some difficulty in building up of intraglottal pressure, especially around the transducer.

A qualification needs to be made here about the combined video and pressure data in Fig. 6. Because a strobe technique was used, it was impossible to obtain sequential video frames during one pressure waveform cycle. To show the contact area better (without obstruction from the pressure transducer), images without the pressure transducer were obtained that had contact profiles similar to those recorded on the VCR. Thus, the video images in Fig. 6 were obtained nonsimultaneously with the pressure signal shown.

There were two observable registers in hemilaryngeal phonation: modal and falsetto. The register shift was distinguishable by the following criteria: Auditorily, falsetto had higher pitch and a breathier quality than modal; visually, falsetto had a smaller mucosa wave amplitude and less contact at the free edge; aerodynamically, falsetto had greater airflows for the same subglottal pressures.

In falsetto register, the impact stress and contact area were negligible. The pressure waveform represented only the aerodynamic pressure during phonation (Fig. 8). This finding agrees with previous observations (25), in which the edges of the vocal folds did not meet at the midline. There is no major collision between the vocal folds in falsetto mode. One would reason, therefore, that falsetto users would have less incidence of nodules. This is supported by some clinical observations. Although there are no empirical data, a previous study (P. W. Wang, 1985, personal communication) resulted in the conclusion that the Qing Yi player, one type of female Chinese opera character who uses only falsetto, has much less chance of developing a nodule than Hua Dan, another type of female Chinese opera character who uses chest voice. Further study on this topic needs to be done in the future.

Intraglottal pressure versus acoustical output

Figure 9 shows the intraglottal pressure waveform and the microphone waveform displayed simultaneously for typical phonation. Also shown in Fig. 9b is an integration of the microphone signal (dashed line), which approximates the glottal flow. Because the microphone was only 10 cm from the glottis, the phase delay due to acoustic propagation is <0.3 ms or ~1/20 of a cycle. The acoustic pressure reaches its minimum value just before vocal fold impact and its maximum value during glottal opening. No vocal tract was attached, and hence a typical formant structure is not seen in the microphone signal. Some ripple is apparent, however, in the impact phase. It is possible that vertical tissue displacement causes a pressure fluctuation.

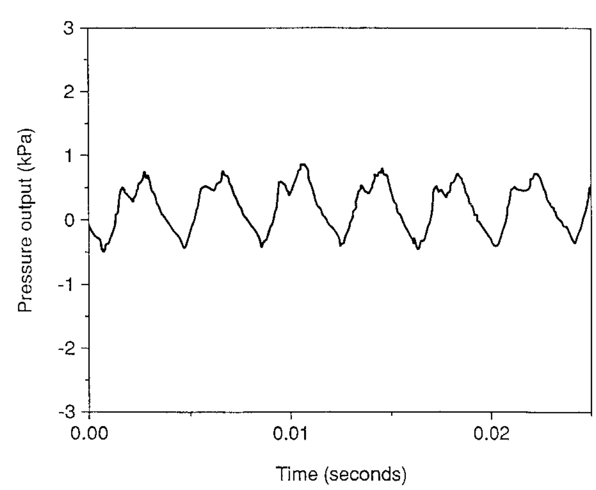

FIG. 8. Intraglottal pressure waveform in falsetto voice. The impact stress peak no longer exists. The pressure waveform represents only the aerodynamic pressure during phonation.

Intraglottal pressure versus subglottal pressure

Figure 10 shows waveforms of the intraglottal pressure waveform at the midpoint of the vocal fold as a function of mean subglottal pressure during modal register, with all the prephonatory settings fixed. Peak impact stress increased as subglottal pressure increased. From these waveforms, Fig. 11 was derived, which is a plot of peak impact stress versus mean subglottal pressure for five larynges. The slope, which is dimensionless (kPa/kPa), varied from 1.1 to 3.8, with an average value of 1.78. This is close to the 2.0 value reported by Scherer and Titze (8).

The question arises: Should the relation between peak impact stress and mean subglottal pressure be linear? In previous work on excised larynges, the amplitude of vibration of the vocal fold was found to vary roughly as the square root of subglottal pressure at constant vocal fold length (26). In this study, the relation between amplitude of vibration and peak impact stress was predicted to be linear (Eq. 6). The combined relation between mean subglottal pressure and peak impact stress should not be expected to be linear, therefore, even though a linear regression line was drawn. More work is needed to tease out the subtleties in variation of A, dx, and Δt in Eq. 6 with mean subglottal pressure. In particular, the impact interval Δt cannot be assumed to be a constant. Nevertheless, our preliminary results support the hypothesis that impact stress is positively related to subglottal pressure and vibrational amplitude.

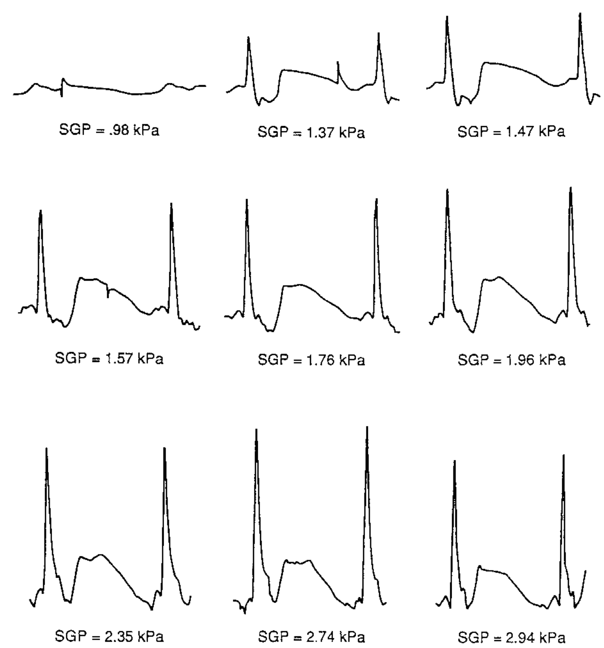

FIG. 10. Intraglottal pressure waveforms at the middle point of the membranous vocal cord (anterior to posterior) at several subglottal pressures (SGP) during normal phonation, with the shim size fixed at 0.5 mm.

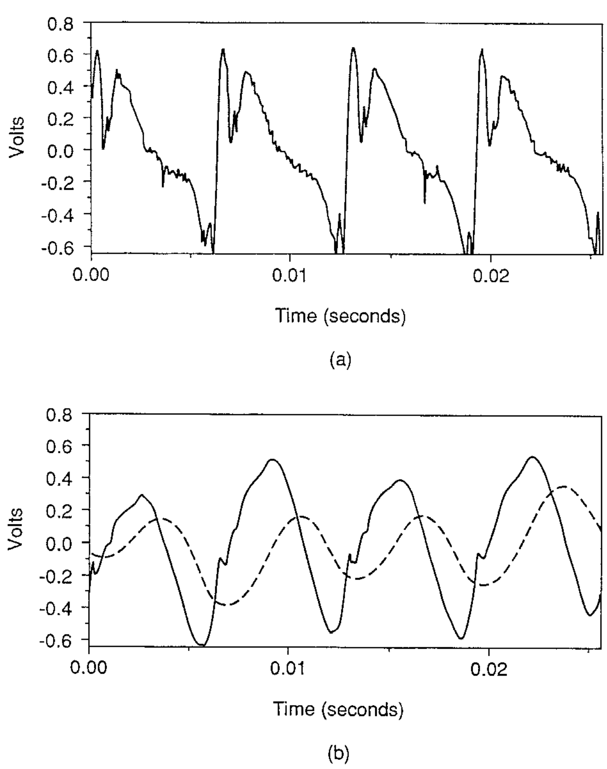

FIG. 9. Simultaneous display of the intraglottal pressure waveform (a) and the acoustic microphone waveform (solid line) (b) in normal phonation. The dashed line is an approximation to the integral of the solid line, representing the glottal flow.

Intraglottal pressure versus vocal fold elongation

Figure 12 shows peak impact stress for different vocal fold elongations during optimal phonation (as defined previously), with adduction at 0.5 mm and subglottal pressure at 1.6–2.0 kPa. In general, vocal fold elongation resulted in an increase in peak stress and a decrease in duration of the peak stress. However, in general, when vocal fold elongation exceeded 5–8%, the peak stress began to decrease again. The effect of vocal fold elongation on the peak impact stress may be a combination of several factors. First, elongation increases the frequency of vibration, thereby increasing the impact force as quantified in Eq. 6. On the other hand, elongation also reduces the amplitude of vibration, thereby possibly decreasing the impact force. If at some length the amplitude reduction becomes more dra-

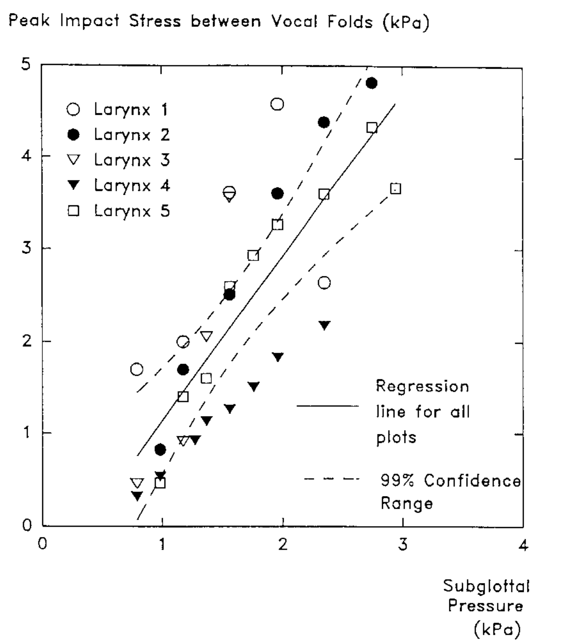

FIG. 11. Relation between peak contact stress and subglottal pressure for five hemilarynges.

matic than the frequency increase, a turning point would be reached as shown.

Intraglottal pressure versus glottal width

Figure 13 shows the intraglottal pressure waveform at three simulated phonation modes: pressed, normal, and breathy. These modes were defined by different glottal widths (shim sizes of −0.5, 0.5, and 1.5 mm, respectively), under constant subglottal pressure and fixed elongation. It appears that pressed voice has the greatest peak impact stress, followed by normal voice and breathy voice, respectively. In Fig. 14, the peak impact stress is plotted as a function of shim size (glottal width). Clearly, the less the glottal width, the greater the peak impact stress. It was also observed that if glottal width was extended to a critical point (typically 1.0–1.5 mm), the vibration mode often switched to falsetto, with a waveform as shown in Fig. 8. Greater elongations usually caused an earlier switch. In contrast, there was no clear switching point between normal voice and pressed voice.

Intraglottal pressure versus location on fold

Peak stresses were measured at three different locations on the vocal fold. Figure 15 shows peak impact stress, normalized to the middle location, for five larynges. In normal phonation, with constant arytenoid approximation, constant vocal fold elongation, and constant subglottal pressure, the peak stresses at the anterior and posterior quarter points of the membranous fold were ~62% of the stress at the midpoint. This corresponds relatively well to the 71% value predicted in Eq. 8, given possible errors in the precise location of vibrational endpoints of the vocal folds and possible deviations from a half-sinusoid model of the lowest string mode.

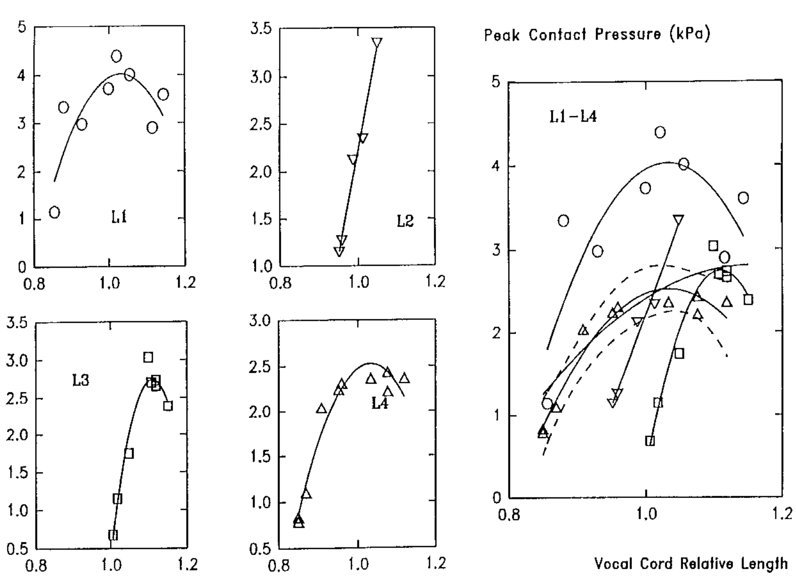

FIG. 12. Peak contact stress versus vocal fold elongation during normal phonation with shim size set at 0.5 mm and subglottal pressure fixed at 1.6–2.0 kPa. **a**: individual larynges; **b**: composite figure (n = 4 larynges).

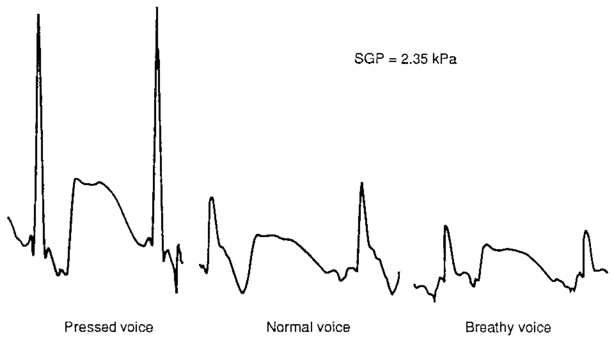

FIG. 13. Intraglottal pressure waveform versus phonation type under constant subglottal pressure (SGP) (2.35 kPa) and 0 elongation.

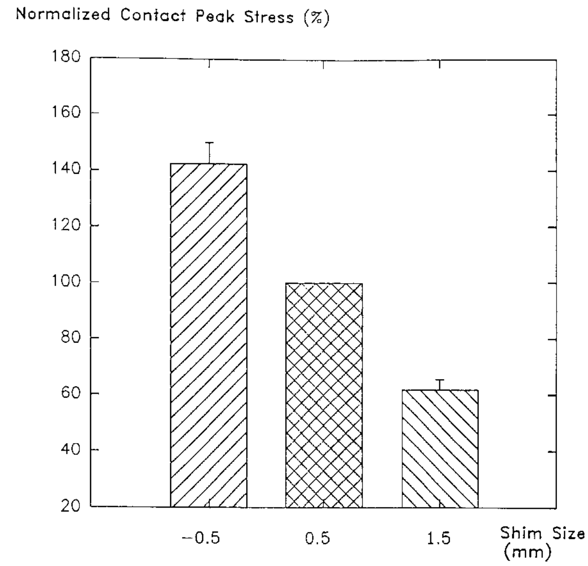

FIG. 14. Peak contact stress versus glottal width (shim size) during phonation under fixed subglottal pressure (1.6–2.0 kPa) and 0 elongation (n = 9 larynges).

CONCLUSIONS, APPLICATIONS, AND LIMITATIONS

The excised hemilarynx procedure offers a method for investigation of impact stress in phonation. In particular, it allows for manipulation of important parameters, such as glottal width, fundamental frequency, and subglottal pressure. It is appropriate to make some further comments regarding clinical applications and future research.

Suggestions for voice abuse and etiology of vocal nodules

According to the present results, higher subglottal pressure, closer distance between the arytenoid cartilages, and greater vocal fold elongation (to a moderate degree) are independently and positively correlated with peak impact stress during phonation. It is also known that subglottal pressure is positively correlated with vocal intensity (27), elongation of the vocal folds with pitch (28), and distance between arytenoid cartilages with "pressing" of the voice (29). Most clinicians assert that loud voice, hyperadduction, and high pitch constitute potentially injurious abuse and misuse of the voice. Therefore, peak impact stress may be a primary factor in vocal abuse and misuse. The present data support the mechanical trauma hypothesis of vocal abuse and vocal nodule etiology.

The mechanical trauma hypothesis is also supported by some histological evidence. Kleinsasser (30) found that tissue regeneration is a major histological finding in vocal nodules. According to Gillman (31), regeneration means replacement of destroyed tissues by connective tissue. Gillman divides the regeneration after an acute trauma into five chronological phases. Because the characteristics of all five regeneration phases can be found in the vocal nodule, Sonninen et al. (15) concluded that traumatic influences extend over a long period of time. Because regeneration occurs after trauma, the implication is that the vocal nodule is caused by trauma. The observation of microstructural changes of a hyperphonated vocal fold (32) also supports the observation that vocal fold trauma occurs after prolonged collisions.

The match between locations of nodules (10,33)

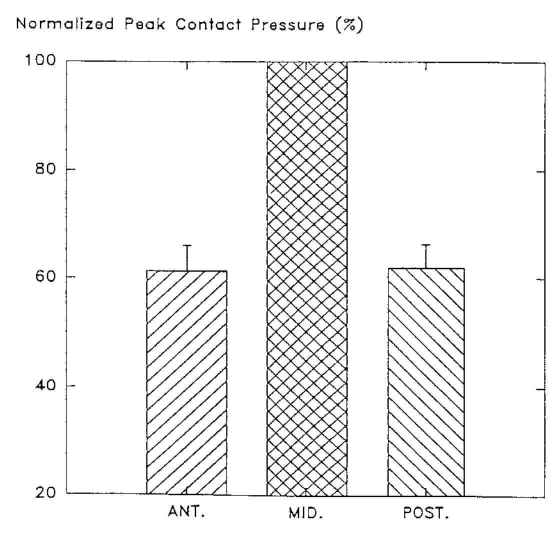

FIG. 15. Normalized peak stress versus anterior–posterior location on vocal fold. The peak stress at the anterior and posterior quarter points of the vocal fold is ~62% of that at the midpoint (n = 5 larynges).

with the location of the maximum impact force also supports the mechanical trauma hypothesis. Both occur at the middle of the membranous fold. An important aspect of voice therapy is to direct patients to talk with less intensity and less adduction and to use appropriate pitch (34). Presumably, the effect is to reduce the impact stress to the midportion of the vocal folds.

Limitation of using the canine larynx

The purpose of the present experiments was to address questions related to human phonation. Canine larynges were used, however. Gross similarities between canine and human larynges allow the canine larynx to be used as a model for studying basic passive mechanisms of human phonation (21, 35–39). In addition to their similarity to human larynges, canine larynges are used because of their availability from other experimental protocols, requiring no additional deaths of vertebrate animals. However, there are some differences between the canine larynx and human larynx (37,39). The most severe limitation is the absence of a vocal ligament in the canine. This difference alone might affect the generalizations made here. In further studies, human larynges might be considered.

Limitation of using a single sensor

As predicted by Ishizaka and Matsudaira (40) and Titze (26,41), intraglottal pressure varies spatially. During our experiments, stress was measured at three different positions by moving a single sensor. This manipulation could cause measurement error. A better solution would be to build an array of sensors to map out pressure distributions in the glottis. Construction details and cost were prohibitive for this experiment. In the future, however, an array could be used to investigate strategies for adjustment of pitch and loudness that yield minimum stress patterns on the colliding tissue.

Acknowledgment: We thank Dr. Ronald C. Scherer for valuable contributions to technical aspects of this article. We also thank Julie Lemke for manuscript preparation and Mark Peters for graphic support. This work was supported by grant no. P60 DC 00976 from the National Institutes of Health.

REFERENCES

1. Jiang J, Titze I. A methodological study of hemilaryngeal phonation. *Laryngoscope* 1993;103:872–82.
2. Cooper DS. Research in laryngeal physiology with excised larynges. In: Cummings CW, ed. *Otolaryngology—head and neck surgery, vol 3.* St. Louis: Mosby, 1986:1766–76.
3. Harless E. Die Stimme. In: Wagner R, ed. *Handwörterbuch der Physiologie, vol 4.* Braunschweig: F. Vieweg und Sohn, 1853.
4. Weiss O. Uber die Entstehung der Vokale. II. Die Vorgange im ausgeschnittenen Kehlkopf. *Arch Exp Klin Phon* 1914;1: 350–5.
5. Scherer RC, Cooper D, Alipour F, Titze IR. Contact pressure between the vocal processes of an excised bovine larynx. In: Titze IR, Scherer RC, eds. *Vocal fold physiology.* Denver: Denver Center for the Performing Arts, 1985:292–303.
6. Murakami Y, Kirchner JA. Reflex tensor mechanism of the larynx by external laryngeal muscles. *Ann Otol Rhinol Otolaryngol* 1971;80:46–64.
7. Murakami Y, Kirchner JA. Mechanical physiological properties of reflex laryngeal closure. *Ann Otol Rhinol Otolaryngol* 1972;81:59–71.
8. Scherer RC, Titze IR. Vocal fold contact stress during phonation. *J Acoust Soc Am* 1982;71(suppl 1):555(A).
9. Reed C, Doherty T, Shipp T. Piezoelectric transducers for the direct measurement of medial forces in the glottis. *J Acoust Soc Am* 1990;88(suppl 1):S151.
10. Nagata K, Kurita S, Yasumoto S, Maeda T, Kawasaki H, Hirano M. Vocal fold polyps and nodules, a 10 year review of 1156 patients. *Auris Nasus Larynx* 1983;(suppl 10):S27–35.
11. Brodnitz FS, Froeschels MD. Treatment of nodules of vocal fold by chewing method. *Arch Otolaryngol* 1954;191:361–3.
12. Lancer JM, Syder D, Jones AS, Boutiller AL. Vocal fold nodules, a review. *Clin Otolaryngol* 1988;13:43–51.
13. Kambic V, Radsel Z, Zargi M, Acko M. Vocal cord polyps: incidence, histology and pathogenesis. *J Laryngol Otol* 1982;95:609–18.
14. Epstein S, Winston P, Friedmann I, Ormerod FC. The vocal fold polyp. *J Laryngol Otolaryngol* 1957;71:673–88.
15. Sonninen A, Damste PH, Jol J, Fokkens J. On vocal strain. *Folia Phoniatr* 1972;24:321–36.
16. Arnold GE. Vocal nodules and polyps: laryngeal tissue reaction to habitual hyperkinetic dysphonia. *J Speech Hear Disord* 1962;27:205–17.
17. Arnold GE. Vocal nodules. *NY St J Med* 1963;63:3096–110.
18. Vaughan CW. Current concepts in otolaryngology: diagnosis and treatment of organic voice disorders. *N Engl J Med* 1982;307:863–6.
19. Gery P. Microlaryngostroboscopy and "singer's nodes." *J Otolaryngol Sol Aust* 1973;3:525–527.
20. Jiang J. Etiology of singer's nodules. A report of EENT Hospital, Shanghai Medical University, Shanghai, China, 1985.
21. Hirano M. Phonosurgery: basic and clinical investigations. *Otologia (Fukuoka)* 1975;21:239–40.
22. Titze IR. A framework of the study of vocal registers. *J Voice* 1988;2:183.
23. Saito S, Fukuda H, Kitahira S, et al. Pellet tracking in the vocal fold while phonating: experimental study using canine larynges with muscle activity. In: Titze IR, Scherer RC, eds. *Vocal fold physiology.* Denver: Denver Center for the Performing Arts, 1985:169–82.
24. Titze IR. Parameterization of the glottal area, glottal flow, and vocal fold contact area. *J Acoust Soc Am* 1984;75:570–80.
25. Rubin HJ, Hirt CC. The falsetto, a high-speed cinematographic study. *Laryngoscope* 1960;70:1305–24.
26. Titze IR. On the relation between subglottal pressure and fundamental frequency in phonation. *J Acoust Soc Am* 1989; 85:901–6.
27. Ishikki N. Regulatory mechanism of voice intensity variation. *J Speech Hear Res* 1964;7:17–29.
28. Hollien H. The relationship of vocal fold length to vocal

pitch for female subjects. Twelfth International Speech and Voice Therapy Conference, Padua. pp. 38–43.
29. Scherer R, Vail V. Measures of laryngeal adduction. *J Acoust Soc Am* 1988;84(suppl 1):S581(a).
30. Kleinsasser O. Pathogenesis of vocal fold polyps. *Ann Otol Rhinol Laryngol* 1982;91:378.
31. Gillman T. Treatise on collagen. In: Gould BS, ed. *Biology of collagen, vol 2*. London: Academic Press, 1968:334.
32. Gray SD, Titze IR, Lusk RP. Electron microscopy of hyperphonated canine vocal folds. *J Voice* 1987;1:109–15.
33. Rubin HG, Lehrhoff I. Pathogenesis and treatment of vocal nodules. *J Speech Hear Disord* 1962;27:150–61.
34. Colton RH, Casper JK. *Understanding voice problems: a physiological perspective for diagnosis and treatment*. Baltimore: Williams & Wilkins, 1990.
35. Koyama T, Harvey JE, Ogura JH. Mechanism of voice production II. Regulation of pitch. *Laryngoscope* 1971;81:47–65.
36. Koyama T, Kawasaki M, Ogura JH. Mechanism of voice production I. Regulation of voice intensity. *Laryngoscope* 1969;79:337–54.
37. Baer T. *Investigation of phonation using excised larynges*. Ph.D. dissertation, Massachusetts Institute of Technology, Boston, MA, U.S.A.
38. Hirano M. Structure and vibratory behavior of the vocal folds. In: Sawashima M, Cooper F, eds. *Dynamic aspects of speech production*. Tokyo: University of Tokyo Press, 1977: 13–27.
39. Kirita S, Nagata K, Hirano M. A comparative study of the vocal folds. In: Bless DM, Abbs JH, eds. *Vocal fold physiology*. San Diego: College Hill Press, 1981:3–21.
40. Ishizaka K, Matsudaira M. Fluid mechanical consideration of vocal fold vibration. Monograph 8, Speech Communication Research Laboratory, Santa Barbara, CA, U.S.A.
41. Titze IR. Comments on the myoelastic-aerodynamic theory of phonation. *J Speech Hear Res* 1980;23:495–510.